CrossMark

Effects of Oxide Scale on the Corrosion and Mechanical Properties for a High Speed Steel and a Graphite Cast Iron

Mitsuhiro Okayasu[1] · **Shaohua Wu**[1]

Abstract The mechanical properties and the oxidation characteristics of the high speed steel (HSS) for hot-rolling process, produced by centrifugal casting process, were investigated experimentally. Because of the complicated microstructure with tiny V-, Cr-, and W-based precipitations in the matrix, high hardness of the HSS samples was obtained. Moreover, high compressive strength and high compressive strain were detected, while low tensile properties were obtained. In spite of the high hardness of HSS, the wear resistance was a low level due to severe oxidation on the HSS surface and generated cracks, but the wear resistance of HSS was still better than conventional graphite cast iron. Although the corrosion occurred by the wear test, no clear microstructural change was detected. Wear and corrosion characteristics were examined at high temperatures and high humidity using an originally proposed testing machine. With this testing machine, failure characteristics of HSS were clarified, in which the HSS sample was worn away easily due to the brittle oxidation scale during the rolling process, leading to the rough HSS surface. Furthermore, the low tensile strength of HSS made an acceleration of the failure especially crack growth. Such rough surface has made reduction in the quality of the rolled materials.

Keywords High speed steel · Oxide scale · Hot-rolling process · Wear property · Mechanical property

✉ Mitsuhiro Okayasu
mitsuhiro.okayasu@utoronto.ca

1 Graduate School of Natural Science and Technology, Okayama University, 3-1-1 Tsushimanaka, Kita-ku, Okayama 700-8530, Japan

🐾 Springer

Introduction

In recent years, hot-rolled steels have been employed for various engineering applications, e.g., automobile and building industries. Strong demand for the hot-rolled steels (final products) is high quality and high material reliability. In particular, high strength and high ductility are required in our industries. Hot rolling is a complicated process, and the quality of the final products is sensitive to the rolling condition. Because of the high compressive stress during the forging process, the surface status of the forging roll die reflects directly the shape of the products. The oxide scale on the die is one of the significant issues, which inevitably grow due to thermal oxidation at elevated temperatures in corrosive environments. Moreover, because of brittle property of the oxide scale, crack generation occurs during the thermal fatigue. The forging roll die, made of graphite cast irons and high speed steels, has been employed widely. Figure 1 displays the schematic and photograph of a forging roll die, made of the high speed steel (HSS). The die has been employed for the actual hot-rolling process for about one month. As seen, the die surface is worn away severely, as indicated by the circle. Cheng et al. have reported that the
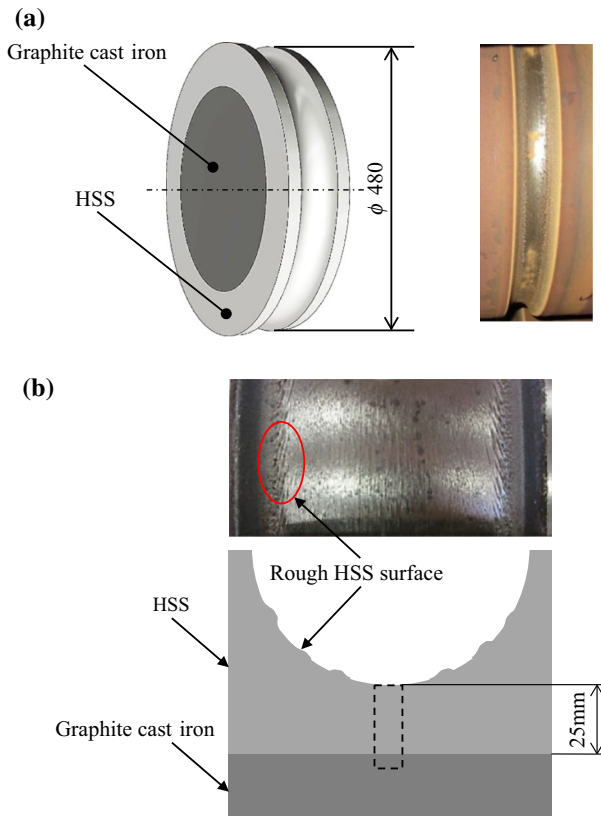

Fig. 1 Schematic and photograph of forging roll die made of high speed steel and graphite cast iron

temperature of the forging process is a significant factor to determine the thickness of the oxide scale and its failure properties [1]. Those occurrences make change of the quality of the final products to deteriorate, where sticking of rolled material occurs by the rough surface of the roll die. The sticking is related to the phenomenon that fragments of the final products are detached and stuck to a die surface [2]. It is also considered that the breaking of oxide scales of the roll die leads to the steel substrate, which counteracts the lubricative effect, resulting in change of the friction coefficient [3]. Metallic oxide scale inevitably grows on the surface of hot-rolled strips because of thermal oxidation with increasing the temperature, and the oxide scale prior to subsequent processing is removed by the forging process [4]. Yu et al. have investigated the microstructure and microtexture evolutions of deformed oxide scale formed on microalloyed steel during the hot rolling and accelerated cooling [5]. Influence of high-temperature hardness and oxidation on sticking phenomena was investigated by Ha et al.: Cr oxides were formed on the surface of the rolled material at 1070 °C, which reduced drastically the sticking due to the increment of the hardness of the forged material. The characterization of the thin oxide scale deformation has been analyzed using the finite element analysis. The oxide scale thickness values, analyzed by FEA, were in good agreement with those obtained experimentally [6]. Yu et al. have conducted electron backscatter diffraction (EBSD) analysis to examine the microstructure and microtexture evolutions of the deformed oxide scale formed on a microalloyed steel during hot-rolling process [5]. Although several investigators have examined the oxide scale characteristics, there is apparently lack of the information regarding the effects of the oxidation on the mechanical and failure properties of the forging roll die. Thus, the aim of the present work is to investigate systematically the fundamental aspects of the oxidation characteristics of the high speed steel in advance using our originally designed testing machine, and the material properties of HSS with and without oxidation were examined. Furthermore, those mechanical properties were compared to those for the graphite cast iron.

Experimental Procedures

Material Preparation

In the present work, HSS and graphite cast iron for the hot-rolling process were employed. Table 1 indicates the chemical compositions of HSS and graphite cast iron. The HSS materials consist of several main alloying elements, e.g., Cr, V, and

Table 1 Chemical composition of high speed steel and graphite cast iron (wt%)

	C	Si	Mn	P	S	Ni	Cr	Mo	W	V	Fe
HSS	1.46	1.08	0.49	0.02	0.01	0.10	3.02	3.09	1.11	3.09	Bal.
Graphite cast iron	3.74	2.68	0.15	0.05	0.02	–	–	–	–	–	Bal.

W, to make high mechanical properties [7, 8]. In this approach, the roll die, formed by round plate of φ480 mm, was made by the centrifugal casting at about 600 rpm, where the outer and the inner materials of the round plate are related to HSS and graphite cast iron, respectively. The round plate was in fact employed for the actual hot-rolling production for about 1 month. After the verification of the failure on the surface of the roll die (Fig. 1), the test samples were cut from the roll die around the surface. The test samples were made directly from the HSS roll die. Moreover, the graphite cast iron samples were prepared to make comparison of the material properties with the HSS ones.

Material Properties

The tensile and compressive properties were examined at room temperature using a screw driven-type universal testing machine with 50 kN capacity. The loading speed for the mechanical tests was fixed at 1 mm/min up to the fracture point. Small dumbbell-shaped specimens (rectangular shapes) were used with dimensions of $4 \times 2 \times 1$ mm for the tensile test. On the other hand, a small rectangular block of $3.5 \times 2 \times 2$ mm was used for the compressive test. In both tests, the relationship between the stress and strain was examined using a data acquisition system in conjunction with a computer through a standard load cell and strain gage.

Hardness of the test samples was investigated by micro-Vickers testers under the following conditions: 0.49 and 98 N for 15 s. Note that, at the low applied load of 0.49 N, the hardness measurement was conducted to the specific microstructural phases, e.g., matrix and eutectic structures.

Microstructural characteristics of HSS and graphite cast iron before and after the wear tests were carried out using optical microscopy, X-ray diffraction (XRD), energy-dispersive X-ray spectroscopy (EDX), and EBSD. For EDX analysis, a JSM-6510 scanning electron microscope (SEM) was employed, and this analysis was conducted with an acceleration voltage of 15 kV. The EBSD analysis was performed with an acceleration voltage of 15 kV, beam current 5 nA, and step size 2 μm using a high-resolution JSM-7001F SEM. The surfaces of the samples for the measurement were polished for about 30 min to mirror level in a vibropolisher.

Failure Characteristics

To understand clearly the failure characteristics of the HSS samples during the hot-rolling process at high temperature and high humidity, wear properties were investigated using a new testing machine developed originally. Figure 2 shows the photograph and the schematic illustration of the testing machine. In this machine, the sample blocks, made of high speed steel and graphite cast iron, were inserted directly to the round plate of 150 mm in diameter and 15 mm in thickness. The sample block was rotated at 100 rpm for various periods of time (5, 10, and 1000 h), in which the sample surface was worn by the loading of about 10 N from the upper direction using a round rod, made of the structural steel (SS400) as shown in Fig. 2. The sample block was heated to about 573 K, which is conducted with heat transfer through a contact with the SS400 rod, heated in the furnace. After the heating, the
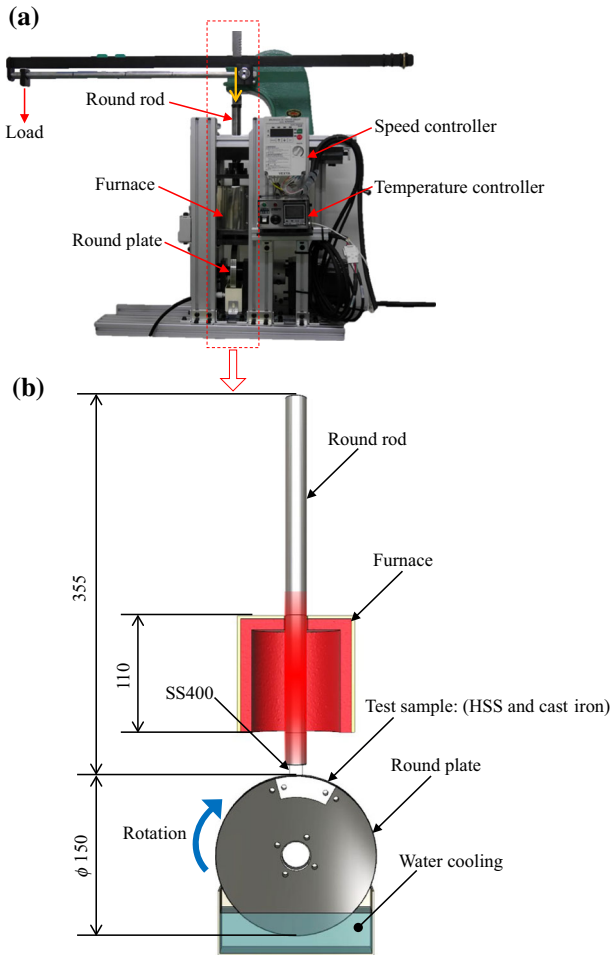
Fig. 2 Photograph and schematic diagram of the wear and corrosion testing machine proposed originally

sample was cooled by cold water, where the sample was immersed directly in the water stored in the related tank. The testing conditions, described above, were designed on the basis of the actual hot-rolling process.

Results and Discussion

Microstructural Characteristics

Figure 3 shows the optical micrographs and EDX analysis of the HSS and graphite cast iron made by the centrifugal casting process. As shown in Fig. 3a, different microstructural characteristics are obtained. The grain size (GS) of the HSS is altered depending on the measurement location due to the different cooling rates,
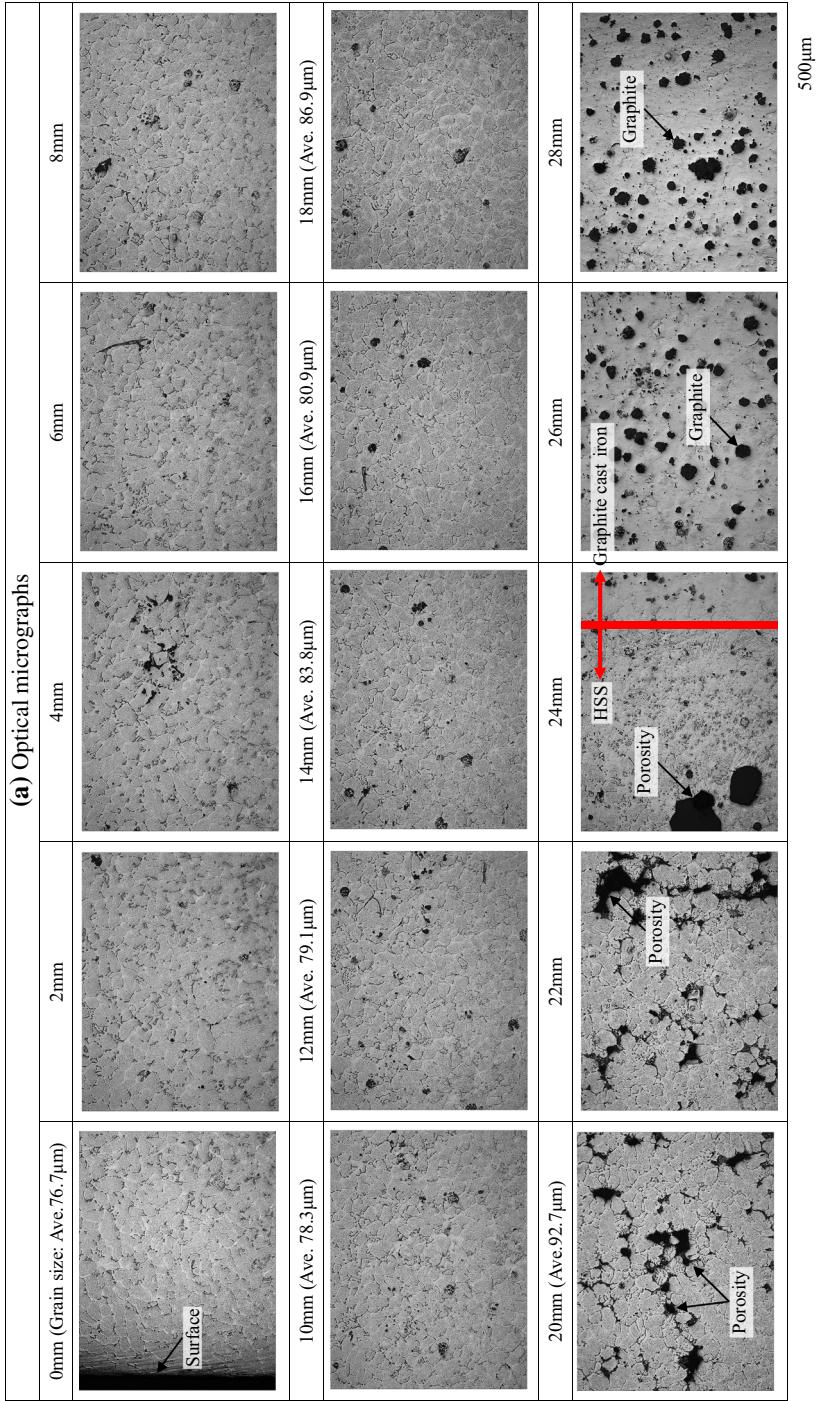
(a) Optical micrographs

◄**Fig. 3** Microstructural characteristics of high speed steel and graphite cast iron: **a**, **b** optical micrographs and **c** EDX analysis
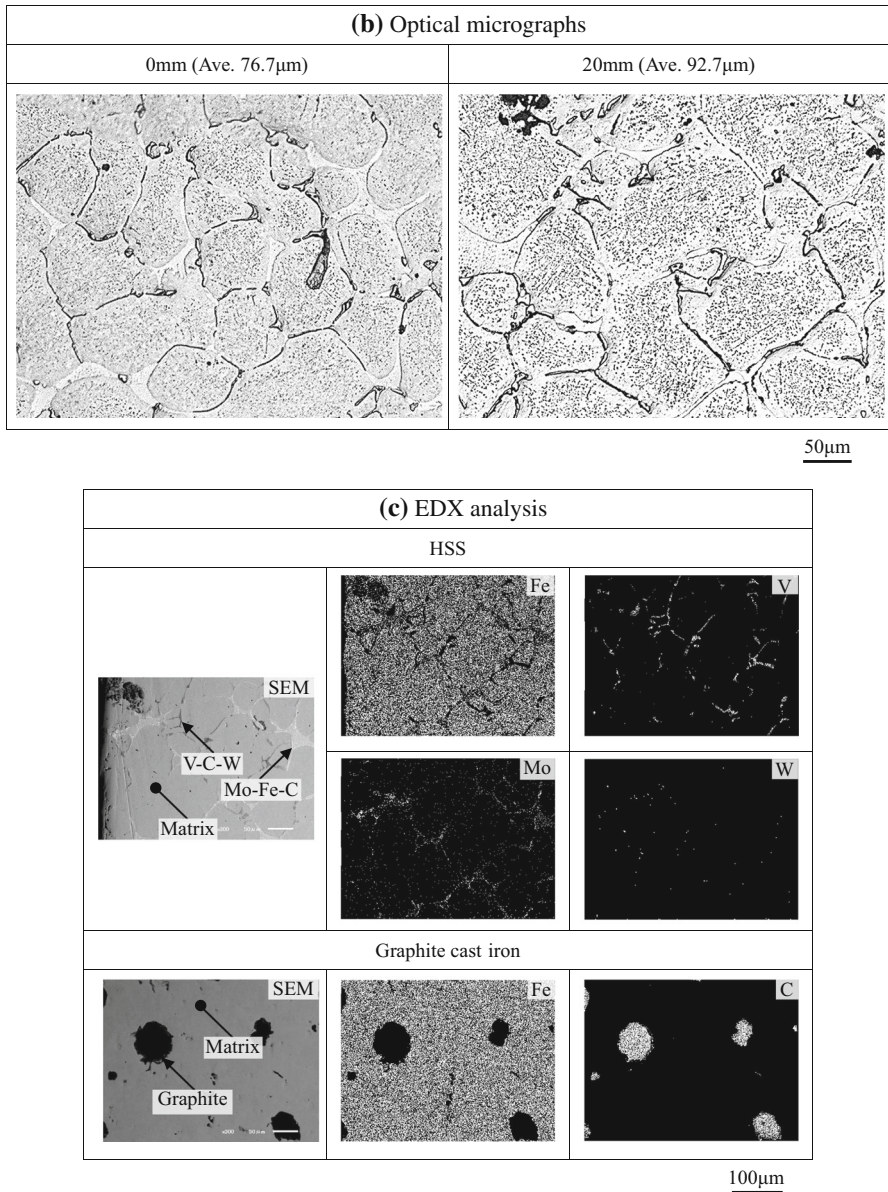

Fig. 3 continued

e.g., Ave. 76.7 µm (near surface) and Ave. 92.7 µm (inside, e.g., 20 mm in depth), see Fig. 3b. Note that the grain size was measured by the manner of straight diagonal lines on each grain. In the area between the HSS and cast iron, a large

amount of porosities is detected, and, in the cast iron, round-shaped graphite phases are obtained. From the EDX analysis (Fig. 3c), it appears that the HSS sample consists of the Fe base matrix with V, W, and Mo precipitate phases. Such complicated structure in HSS may lead to the high mechanical properties [9]. Figure 4 shows the variation of the grain size as a function of the measurement location from the sample surface. Although the obtained data are relatively scattered, the grain size increases nonlinearly, where correlation rate is about $R^2 = 0.49$.

Figure 5 shows the variation of the Vickers hardness for the HSS and cast iron samples. The hardness of HSS adjacent to its surface is about 580Hv, and that level decreases slightly with increasing the distance from the surface of HSS, e.g., less than 450Hv in the HSS sample near the cast iron, e.g., at 20 mm from the surface. This could be attributed to the change of the microstructure caused by the different solidification rates during the centrifugal casting, e.g., the smaller the grain, the higher the hardness. On the other hand, widely scattered hardness is observed in the HSS near the cast iron due to many defects; moreover, a considerable drop in the hardness is obvious in the graphite cast iron, where the mean hardness is about 300Hv. Figure 6 displays the relationship between the grain size and hardness of the HSS sample. As seen, there is almost linear relationship between GS and hardness at the correlation rate of $R^2 = 0.58$, e.g., Hv = −5.8GS (μm) + 1107.3. Note that the hardness values in the HSS matrix and vanadium base eutectic phases of HSS measured are about 450Hv and more than 1000Hv, respectively, and low hardness of approximately 25Hv is obtained in the round graphite of the cast iron.
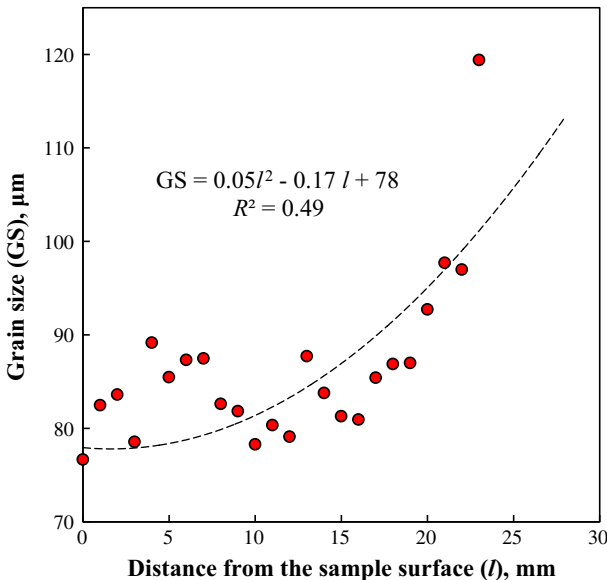

Fig. 4 Relationship between the grain size and measurement location of high speed steel
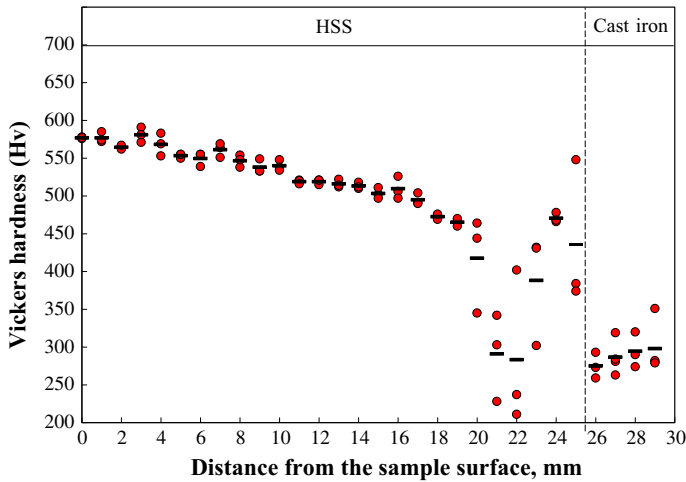
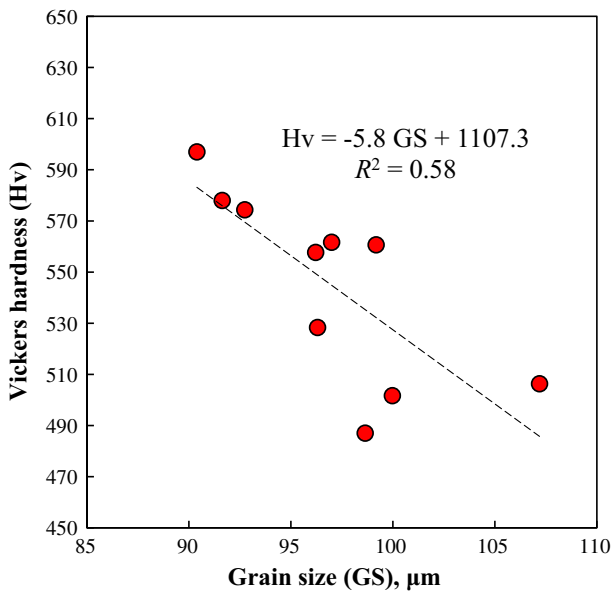**Fig. 5** Variation of the Vickers hardness of high speed steel and graphite cast iron


$$Hv = -5.8 \, GS + 1107.3$$
$$R^2 = 0.58$$

Fig. 6 Relationship between the grain size and hardness

Mechanical Properties

Figure 7a shows the representative stress versus strain curves for HSS, examined at room temperature, and their mechanical properties are summarized in Fig. 7b. Note that, in this approach, four test specimens were employed to obtain reliable data. It is clear that there is a linear relationship between tensile stress and tensile strain

Fig. 7 Mechanical properties of high speed steel at room temperature: **a** Representative stress–strain curves for the tensile and compressive tests, **b** ultimate strengths and fracture strains
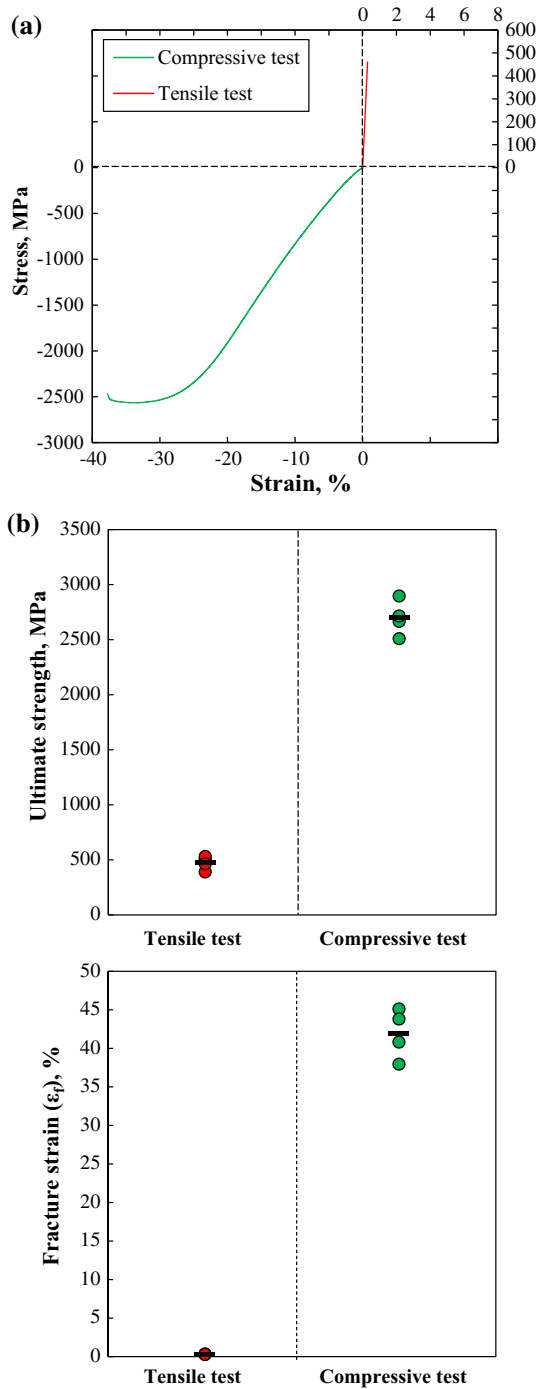
with the high elastic constant until final failure, which would be arising from the high hardness. It is considered from the tensile properties that no severe plastic deformation could have occurred. The ultimate tensile strength of HSS is appeared to be about 490 MPa. Moreover, the fracture tensile strain (ε_f) is as low as 0.35%. Pavlina and Tyne have introduced the linear relationship between Vickers hardness and ultimate tensile strength (σ_{UTS}) of the related steels, e.g., $\sigma_{UTS} = -99.8 + 3.734Hv$ [10]. On the basis of this equation and hardness data of HSS, obtained as about 500Hv (Fig. 5), the tensile strength of HSS can be estimated as 1767.2 MPa: $\sigma_{UTS} = -99.8 + 3.734 \times 500$. The estimated σ_{UTS} value is more than three times higher than that for the experimentally obtained σ_{UTS} one (490 MPa). In contrast, high compressive strength (σ_{UCS}) and high compressive strain of HSS (ε_f) were detected, e.g., $\sigma_{UCS} = 2800$ MPa and $\varepsilon_f = 42\%$, where the lower elastic constant for the compressive stress–strain is obtained. Because the severe permanent strain is obtained, severe work hardening may have occurred despite of the high hardness material. This occurrence will be discussed in the later section of this paper. In addition, an attempt was made to examine the compressive properties of HSS at 773 K. From this test, it appeared that the compressive strength of HSS at the high temperature is almost same level of that examined at room temperature, $\sigma_{UCS} = 2900$ MPa, as shown in Fig. 7b. It should be noted that, in this approach, the heated sample in furnace was taken out to the testing machine stage, so the temperature decrement of the sample could have occurred slightly during the compressive test.

Figure 8 displays the SEM images of the fracture surfaces for the HSS specimens after the tensile and compressive tests at room temperature. As seen, brittle feature of cleavage is dominated failure for the tensile test specimen, resulting in the low tensile properties. On the contrary, slip failure, caused by the maximum shear stress, is observed for the compressive test one, where many slip lines on the fracture surface are detected. Note that such fracture modes are similar to those for the sample tested at the high temperature.

Failure Mechanism

To understand the failure and corrosion characteristics of the HSS sample after the actual forging process (for about 1 month) as well as our experiment (for 1000 h) using our testing machine (Fig. 2), EDX analysis of both HSS samples after the experiments was conducted in the cross section of the sample near the surface. Figure 9a shows the SEM images and EDX analysis of the HSS samples. As seen in the HSS sample after the forging process (roll die), rough surfaces with dark regions and several major cracks can be obtained. Such dark area is also similarly seen in our test HSS sample, Fig. 9b. It is clear from the XRD analysis that the dark regions are related to the oxide scale: their thickness and the amount of oxide content in the associated area are about 0.05 mm and about 30%, respectively. It has been reported that Al_2O_3 and Cr_2O_3 scales are formed during the heating around 1273 K on the surface of $Fe–Cr_{18}–Al_5$ and $Ni–Cr_{25}$ base alloys, respectively [11]. Despite Cr element in our HSS, Cr base scales could not be detected in our XRD analysis. On the other hand, similar oxide layer can be seen in the related work by Chen and
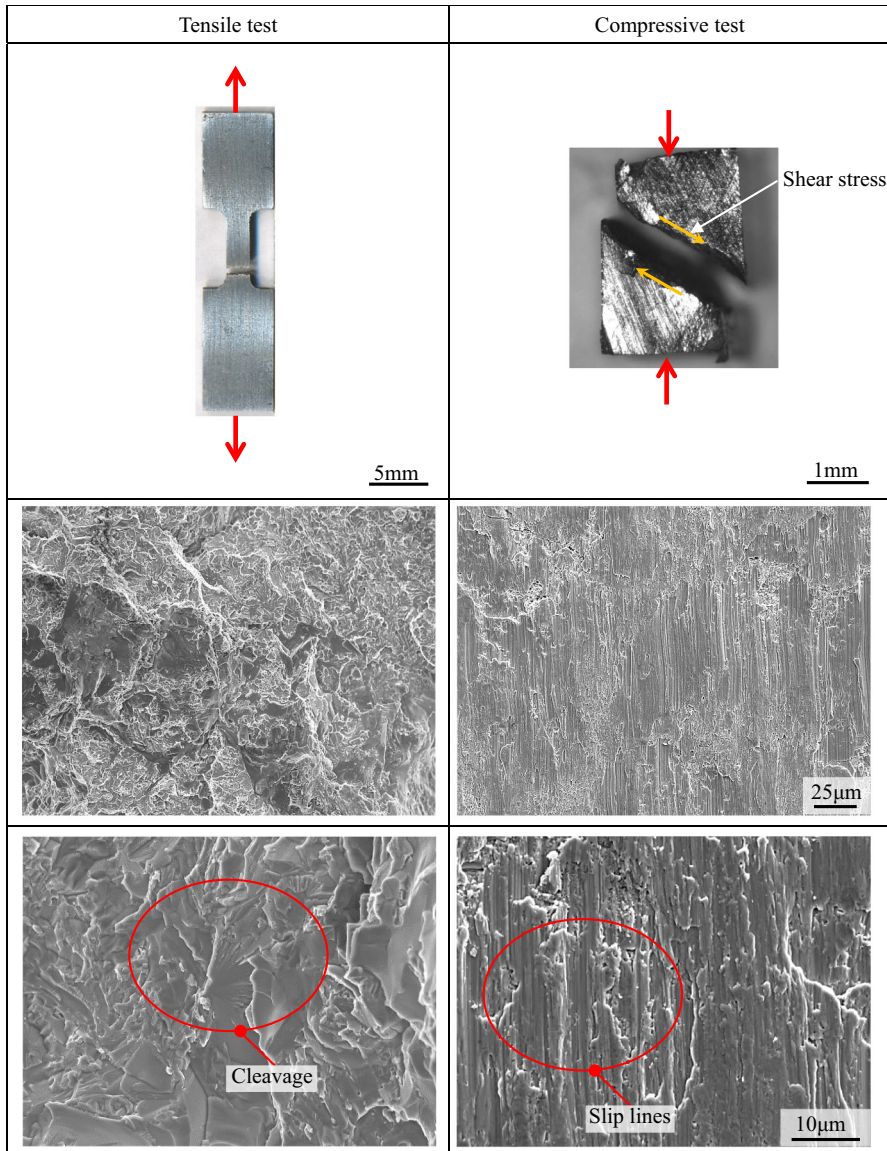
Tensile test	Compressive test
5mm	Shear stress 1mm
	25μm
Cleavage	Slip lines 10μm

Fig. 8 SEM images of fracture surfaces for high speed steel after the tensile and compressive tests at room temperature

Yuen, where the oxide scale structure is formed on commercial hot-rolled steel strip [12]. They have introduced the mechanism of the oxide layer formation, which is related to Fe_2O_3 and Fe_3O_4. It is considered from this result that the oxidation characteristics for the actual hot-rolling process are similarly made by our original testing machine. However, no clear cracks are detected in our test samples. This may be caused by the low applied load of about 10 N. Interestingly, such oxide
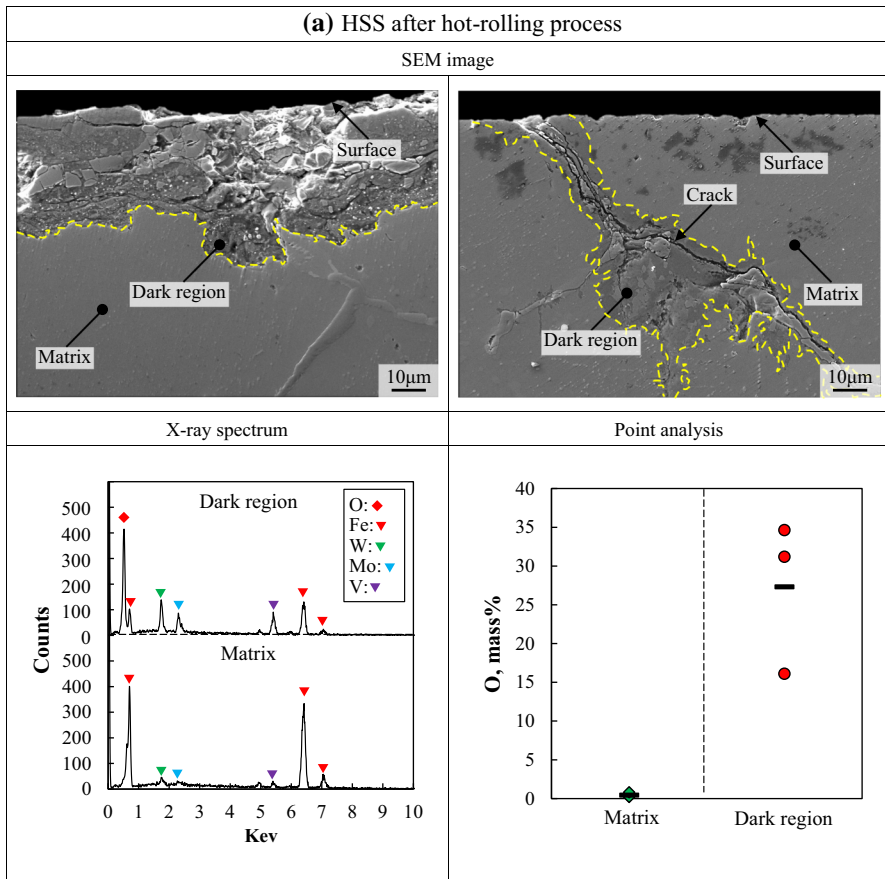
Fig. 9 SEM and EDX analysis of high speed steel after the hot-rolling process and the reproducible experiment

layer is also observed around the cracks for the roll die, Fig. 9a [13, 14]. As the oxide scale has a brittle property, this region could be removed easily by the wear process (during the forging process). Hence, the oxidation area could be worn away, leading to the rough HSS surface (Fig. 1). This occurrence could be summarized by the schematic illustration in Fig. 10.

To further interpret the corrosion and erosion wear characteristics of the HSS samples, the associated tests were carried out for HSS and cast iron using our testing machine under various conditions. The testing conditions in details are as follows: the test samples were rotated with (a) only immersing in water; (b) wearing with heated rod without water cooling; and (c) wearing with heated rod and immersing in water.

Figure 11 depicts the SEM images of the HSS and cast iron after the corrosion tests for 10 h. As seen, weak corrosion is seen in both HSS and cast iron by wearing without water cooling [condition (b)]. The sample oxidation is observed slightly
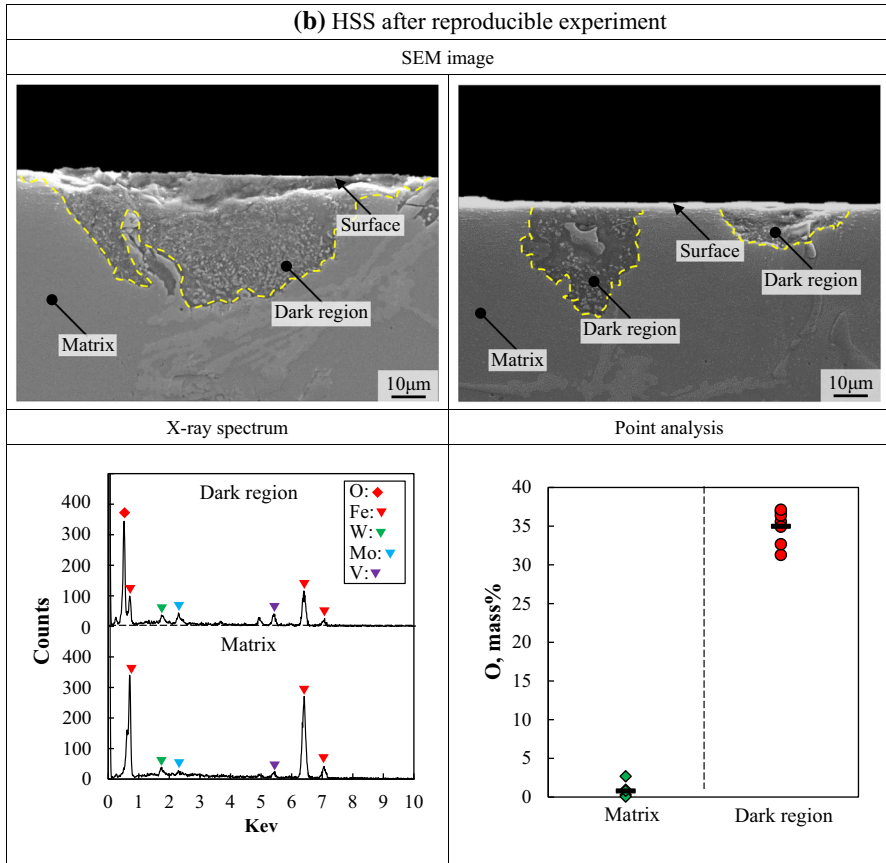
Fig. 9 continued

around the surface of the graphite cast iron due to the immersing in water, but no clear corrosion is seen for the HSS sample [condition (a)]. From this, the HSS sample could have the higher corrosion resistance compared to the graphite cast iron. The oxidation occurred similarly in both samples by the wearing and immersing in water [condition (c)]. It could be understood from this approach that the failure on the forging die surface can occur in HSS, even if the forging process is conducted for a short period of time (10 h).

The wear characteristics under condition (b) and (c) were further investigated for both HSS and cast iron, and the obtained results are displayed in Fig. 12. It is obvious that in the wear tests for 5 h (Fig. 12a), the wear amount for the cast iron is higher than that for the HSS one in both conditions (b) and (c), which is due to the low material hardness for the cast iron. In addition, severe erosion wear occurred in both samples as tested with immersing in water, compared to the dry condition. This could be attributed to the oxidation of the sample, as described above. Figure 12b shows the variation of the weight loss of HSS as a function of the wearing time. As seen, the weight loss increases with increasing the wearing time, while the slope of
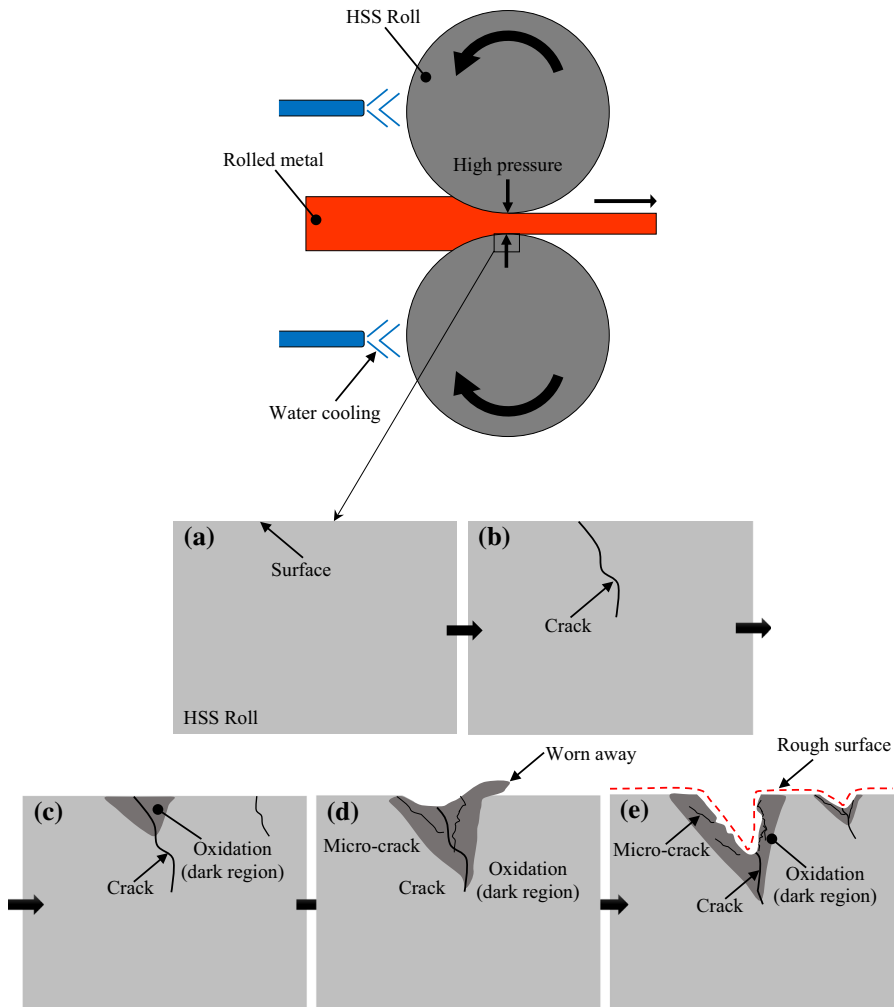
Fig. 10 Model for the wear mechanism of the HSS samples during the hot-rolling process

the weight reduction is different depending on the testing condition, e.g., the severe erosion wear occurs as the sample is worn with immersing in water. This could be affected by the strong corrosion (oxidation) of HSS.

To understand the change of the material properties after the wear tests, the hardness measurement of the HSS and graphite cast iron sample near the wear and corrosion region was executed. The obtained results are indicated in Fig. 13. As seen, slight increment of the hardness for HSS is seen after the wear test with water. This may be due to the work hardening. In contrast, material softening occurred relatively for HSS after the wear test without water. On the other hand, significant change of the hardness is obvious for the graphite cast iron compared to that for the HSS ones. From this result, it is considered that the microstructural formation
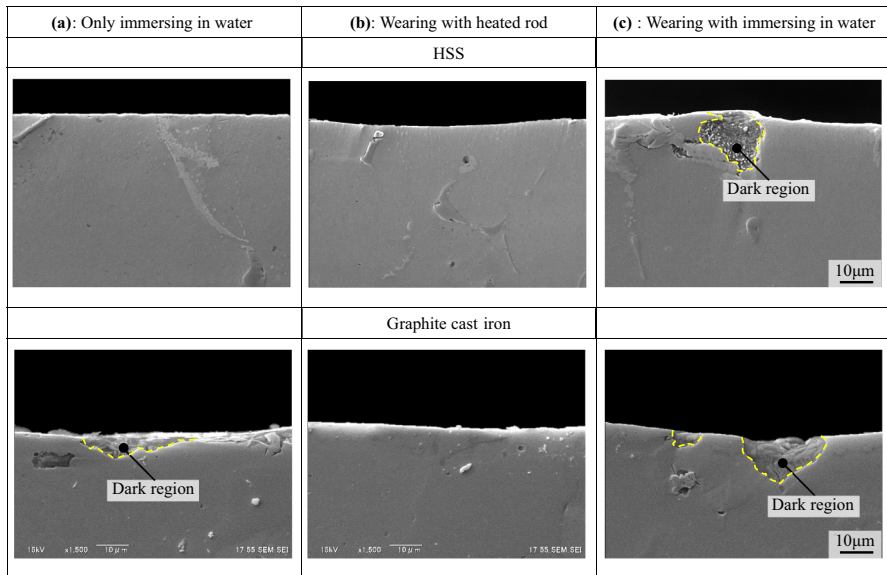
(a): Only immersing in water	(b): Wearing with heated rod	(c): Wearing with immersing in water
	HSS	
	Graphite cast iron	

Fig. 11 SEM images of high speed steel and graphite cast iron after wear and corrosion tests for 10 h under various conditions: **a** only immersing in water, **b** wearing with heated rod without water cooling, and **c** wearing with immersing in water

cannot be changed significantly for the HSS sample after the wear tests compared to the graphite cast iron one.

The microstructural characteristics after the wear tests were examined by EBSD analysis. Figure 14 displays the inverse pole figure (IPF), misorientation (MO), and phase maps of various HSS samples. Note that, in this case, the EBSD analysis was also conducted for HSS after the compressive test, because of the severe permanent deformation as mentioned previously. It is clear from Fig. 14 that the microstructural characteristics (misorientation angle and phase structure) for the HSS sample after wear tests were not altered significantly, while severe deformation with the high MO angle, i.e., high internal strain, is detected for the compressive test sample. Thus, it is convinced that the microstructural change would not occur in the HSS sample by the wear tests. It is interest to note that slight increment of austenite phase is observed for the HSS sample after the compressive test, which infers that strong deformation can change the phase structure. However, further study will be required in the future.

Conclusions

The mechanical properties and the oxidation characteristics of the high speed steel and graphite cast iron produced by centrifugal casting process have been experimentally investigated. The results obtained are as follows:

Fig. 12 a Weight loss of high speed steel and graphite cast iron after the wear tests: wearing with and without water cooling for 5 h, and b variation of the weight loss as a function of wearing time for high speed steel
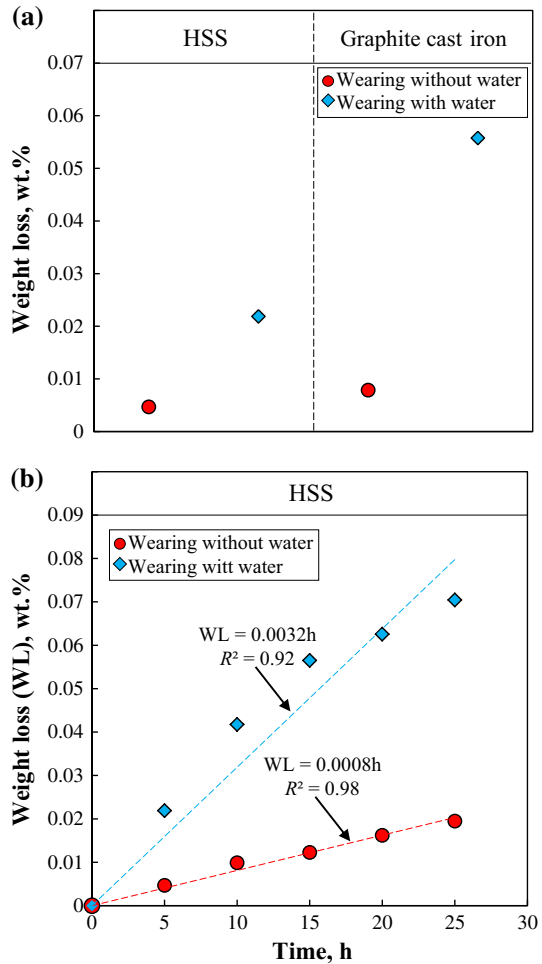
(1) New testing machine has been originally produced to understand the failure characteristics of the rolled die. With this testing machine, erosion wear and corrosion characteristics were investigated at high temperatures and high humidity.

(2) The failure on the surface of HSS samples occured during the hot-rolling process for about one month, where the surface of HSS was worn away due to the oxidation of the samples. The oxidation was not only created on the surface of HSS but also made around the crack generated from the sample surface. Because of the brittle properties of the oxide scale, the oxidation area could be removed easily during the rolling process. The oxide layer was found to be about 0.05 mm in thickness. From EDX analysis, amount of oxide element in the oxide scale was approximately 30%.

(3) Similar oxidation characteristics of HSS were obtained by the experiment using our original testing machine, although no clear cracks were detected.

Fig. 13 Vickers hardness of
high speed steel and graphite
cast iron near the surface regions
before and after the wear tests
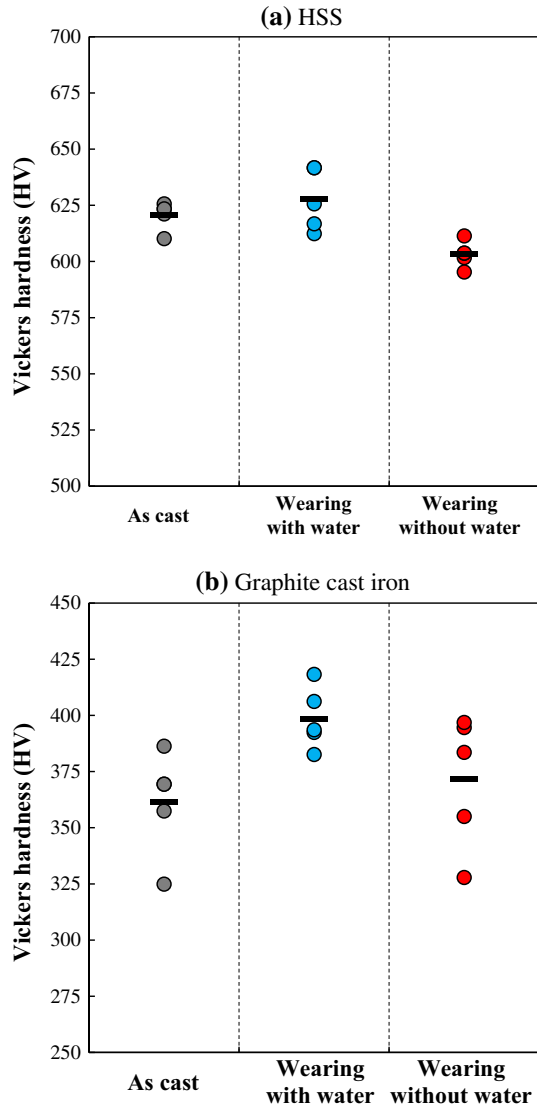
This is due to the low applied load. Such oxidation could occur even if the experiment with a short period of times (10 h). The corrosion resistance of HSS was higher than that for graphite cast iron.

(4) High compressive properties and high hardness of the HSS samples were obtained despite the low tensile properties. The high hardness could be attributed to the complicated microstructural characteristics with tiny precipitated V, Cr, and W phases in the matrix. However, the low tensile properties made an acceleration of its failure and corrosion around the cracks.
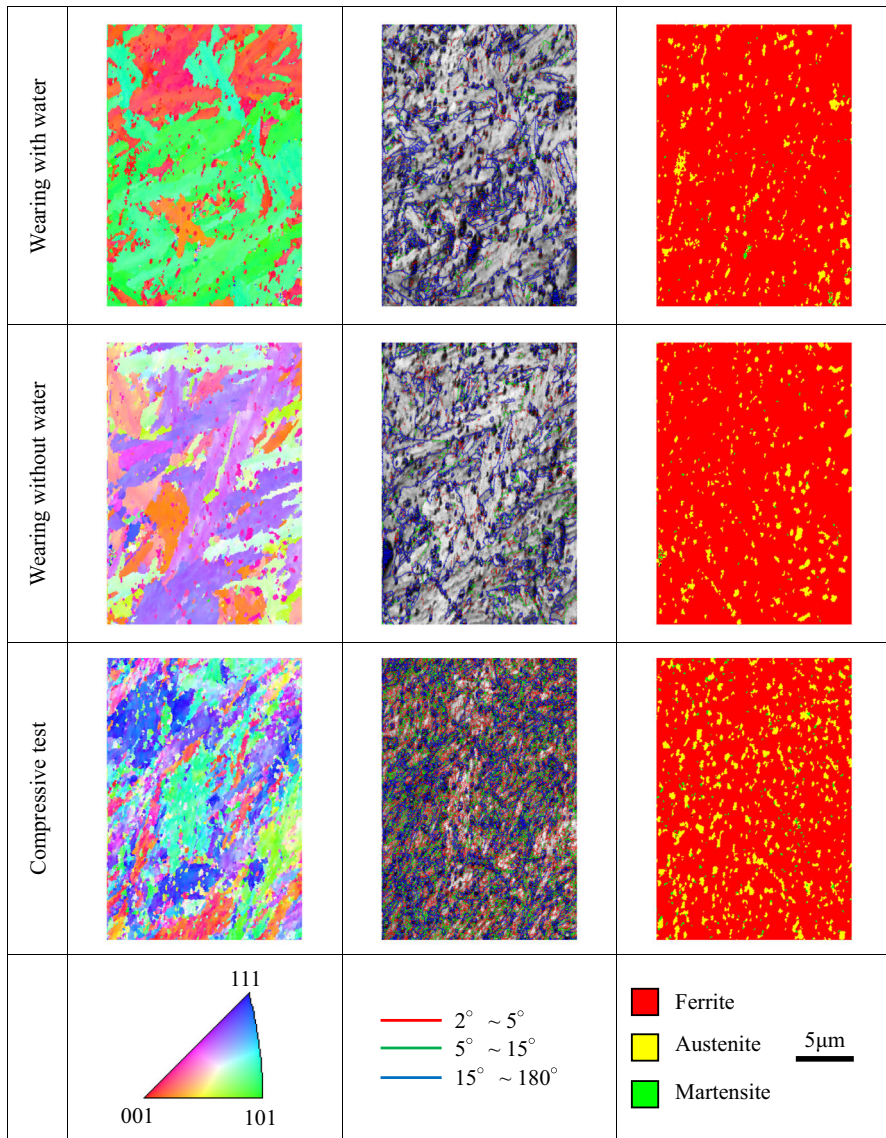
Fig. 14 EBSD analysis of high speed steel before and after the wear and the compressive tests (IPF, MO and Phase maps)

(5)   The wear amount for the graphite cast iron was higher than that for the HSS sample because of the different material hardnesses. Severe erosion wear occurred for both cast iron and HSS samples as wear tests were conducted with immersing in water compared to the dry condition. This could be influenced by the oxidation of the sample surfaces. The wear amount increased linearly with increasing the testing time for HSS. Microstructural

change of the HSS samples was not clarified after the wear test, although severe deformation with high internal strain is detected after the compressive test, where compressive strain is more than 40%.

References

1. X. Cheng, Z. Jiang, J. Zhao, D. Wei, L. Hao, J. Peng, M. Luo, L. Ma, S. Luo and L. Jiang, *Wear* **338–339**, 178 (2015).
2. D. J. Ha, C.-Y. Son, J. W. Park, J. S. Lee, Y. D. Lee and S. Lee, *Materials Science and Engineering A* **492**, 49 (2008).
3. D. B. Wei, J. X. Huang, A. W. Zhang, Z. Y. Jiang, A. K. Tieu, X. Shi and S. H. Jiao, *Wear* **271**, 2417 (2011).
4. M. Krzyzanowski, J. H. Beynon and D. C. J. Farrugia, *Oxide scale ehavior in high temperature metal processing*, (WILEY-VCH Verlag GmbH & Co. KGaA, Weinheim, 2010).
5. X. Yu, Z. Jiang, J. Zhao, D. Wei, C. Zhou and Q. Huang, *Corrosion Science* **90**, 140 (2015).
6. Z. Y. Jiang, A. K. Tieu, W. H. Sun, J. N. Tang and D. B. Wei, *Materials Science and Engineering A* **435**, 434 (2006).
7. A. Benazza, A. Ziadi, B. Serier, B. B. Bouiadjra and B. Boutabout, *Journal of Materials Science* **42**, 834 (2007).
8. H. Fu, Y. Qu, J. Xing, X. Zhi, Z. Jing, M. Li and Y. Zhang, *Journal of Materials Engineering and Performance* **17**, 535 (2008).
9. S. Lee, K. S. Sohn, C. G. Lee and B. I. Jung, *Metallurgical Material Transactions A* **28A**, 123 (1997).
10. E. J. Pavlina and C. J. Van Tyne, *Journal of Materials Engineering and Performance* **17**, 888 (2008).
11. P. Y. Hou and J. Stringer, *Oxidation of Metals* **38**, 323 (1992).
12. R. Y. Chen and W. Y. D. Yuen, *Oxidation of Metals* **56**, 89 (2001).
13. J. W. Park, H. C. Lee and S. Lee, *Metallurgical and Materials Transactions A* **30A**, 399 (1999).
14. Y. J. Kang, J. C. Oh, H. C. Lee and S. Lee, *Metallurgical and Materials Transactions A* **32A**, 2515 (2001).